# Combined analysis of chromatin accessibility, promoter interactions and whole genome sequencing solved the missing heritability in gastric cancer

São José C.[1,2], Ferreira M.[1,3], Cordova L.[4], Pedro A.[1], Senz J.[5], Garcia-Pelaez J.[1,2], Lobo S.[1,6], Gullo I.[1,7,8], André A.[1], Kaurah P.[5], Puntieri F.[9], Glaser J.[9], Huntsman D.[5,10,11], Mundlos S.[9,12,13], Schrader K.[4,14], Oliveira C.[1,8]

[1] Instituto de Investigação e Inovação em Saúde, University of Porto, Porto, Portugal

[2] Doctoral Programme in Biomedicine, Faculty of medicine, University of Porto, Porto, Portugal

[3] Department of Computer Science, Faculty of Science, University of Porto, Rua do Campo Alegre s/n, 4169-007 Porto, Portugal

[4] Department of Medical Genetics, University of British Columbia, Vancouver, British Columbia, Canada

[5] Department of Pathology and Laboratory Medicine, University of British Columbia, Vancouver, British Columbia, Canada

[6] ICBAS -School of Medicine and Biomedical Sciences of the University of Porto, Porto, Portugal

[7] Department of Pathology, Unidade Local de Saúde de São João, Porto, Portugal

[8] Faculty of Medicine of the University of Porto, Porto, Portugal

[9] Max Planck Institute for Molecular Genetics, Berlin, Germany

[10] Department of Molecular Oncology, British Columbia Research Institute, Vancouver, British Columbia, Canada

[11] Genetic Pathology Evaluation Centre, University of British Columbia and Vancouver General

[12] Institute of Medical and Human Genetics, Charité Universitätsmedizin Berlin, Berlin, Germany

[13] Berlin-Brandenburg Center for Regenerative Therapies (BCRT), Charité Universitätsmedizin Berlin, Berlin, Germany

[14] Hereditary Cancer Program, BC Cancer, Vancouver, Canada

***Correspondence:** Carla Oliveira, BSc, PhD; Email: carlaol@i3s.up.pt; Phone +351-225570785

**Abstract**

Missing heritability in hereditary diffuse gastric cancer (HDGC) ranges from 60 to 90%. These HDGC-like families, despite complying with HDGC clinical criteria, lack *CDH1* and *CTNNA1* actionable germline variants, and are not offered HDGC-targeted life-saving disease prevention measures. Herein, we explored novel HDGC predisposition mechanisms affecting the *CDH1*-regulatory network. We called single-nucleotide (SNV) and copy-number variants (CNV) from 19 HDGC-like probands from whole-genome sequencing data and performed gene-ontology analysis. Chromatin enhancer marks and *CDH1* promoter interactions were evaluated in normal stomach by ChIP-seq, ATAC-seq and 4C-seq, variant causality was assessed by RT-PCR, immunohistochemistry and microsatellite instability (MSI) analysis in tumours. Functional analysis was performed using CRISPR-Cas9, RT-PCR and flow cytometry in cell lines, and enhancer assays using mouse embryos. Within the *CDH1* topologically associating domain (TAD), we found two deletions in Family F4 and F9. F4 carried a heterozygous *CDH3* 20kb-CNV triggering *CDH1* mRNA/protein loss in homozygosity by CRISPR-Cas9 editing, similarly to a *CDH1* coding deletion. This 20kb sequence encloses two hypomorphic tissue-specific regulatory elements (REs), each contributing 50% to *CDH1* expression regulation. F9 carried a heterozygous 39bp-intergenic CNV downstream of *CDH1*, triggering *CDH1* mRNA/protein loss by CRISPR-Cas9. F15, presenting gastric but not colorectal cancer, carried an *MLH1* heterozygous 2.7Kb germline CNV overlapping a stomach-specific RE found by ChIP-seq. The gastric tumour of mixed histology displayed Microsatellite instability (MSI), reduced *MLH1* mRNA and protein, and reduced *CDH1* and E-cadherin protein. CRISPR-Cas9 clones mimicking the *MLH1* heterozygous CNV, triggered loss of *MLH1* and *CDH1*/E-cadherin mRNA and protein, similar to a coding deletion. Beyond the *CDH1* TAD and tumour risk syndrome genes, multiple deletions of stomach accessible chromatin sequences were found in particularly young-affected individuals from additional 6 families. This oligogenic pattern impaired specifically mucin genes and multiple immune-related pathways. Herein, we pinpointed novel mechanisms behind HDGC predisposition. One involves deletions of *CDH1*-REs in the TAD or stomach-specific *CDH1*-REs in the *MLH1* locus. The second involves multiple deletions of stomach REs affecting mucin and immune-related genes, favouring a gastric immune-deficient phenotype. Altogether, by combining stomach-specific chromatin accessibility and promoter interactions with whole genome sequencing, we solved the missing heritability in 47% of HDGC-like families within our cohort.

## Introduction

Missing heritability in hereditary diffuse gastric cancer (HDGC) ranges from 60 to 90%. This corresponds to the proportion of families, that despite complying with clinical criteria for HDGC (Blair et al. 2020), cannot be explained by genetic variants in *bonafide* HDGC-associated genes, *CDH1* (ENSG00000039068) and *CTNNA1* (ENSG00000044115), and are called HDGC-like (Oliveira et al. 2009b; Blair et al. 2020). While 10- 40% of HDGC families bear heterozygous coding truncating variants (actionable) in *CDH1* (Oliveira et al. 2009b, 2015), only 2% carry *CTNNA1* truncating variants (Lobo et al. 2021). HDGC-like families remain genetically undiagnosed, even after deep analysis using candidate gene, whole exome and whole genome sequencing (WGS) (Hansford et al. 2015; Oliveira et al. 2015; Tedaldi et al. 2019).

Carriers of actionable variants in *CDH1* have increased risk for early-onset diffuse gastric cancer (DGC) and lobular breast cancer (LBC), the HDGC-associated phenotypes (Guilford et al. 1998; Oliveira et al. 2009a; Garcia-Pelaez et al. 2023). Truncating SNVs in *CTNNA1* have also been associated with DGC predisposition in a small fraction of HDGC families (Majewski et al. 2013; Lobo et al. 2021). Complete *CDH1* and *CTNNA1* loss of function, due to somatic inactivation of the remaining wild-type allele, results in loss of cell adhesion, disruption of epithelial architecture and decreased differentiation, features of signet-ring cells characteristic of HDGC-related tumours (Oliveira et al. 2009c; Benusiglio et al. 2019; Gullo et al. 2020).

Identification of *CDH1* and *CTNNA1* actionable variants in families fulfilling HDGC clinical criteria, triggers cascade genetic testing and intensive surveillance through endoscopy with multiple biopsies, and/or prophylactic gastrectomy in asymptomatic carriers. For asymptomatic *CDH1* female carriers breast intensive surveillance using magnetic resonance imaging (MRI) and computed tomography scan (CT-scan) is recommended, alongside the option of (Blair et al. 2020).

Missing heritability hampers the use of personalized life-saving measures, and may lead to prophylactic surgery in individuals lacking genetic diagnosis, solely based on family history (São José et al. 2023a). HDGC-like families, clinically undistinguishable from *CDH1*-HDGC families, often exhibit germline mono-allelic *CDH1* RNA expression in normal tissues and loss of E-cadherin expression in tumours, despite the lack of germline coding SNVs or CNVs in *CDH1* (Pinheiro et al. 2010). These observations pinpoint a likely causality for *CDH1* and argues towards the presence of undiagnosed germline alterations within noncoding *cis*-regulatory elements (REs), controlling *CDH1* expression and function.

Enhancer-promoter communication within the nucleus tightly regulates cell-type-specific gene expression (Spielmann et al. 2018). REs are instrumental for proper gene expression in time and space and enhancers in particular, play an important role in controlling expression of disease-causing genes (Cova et al. 2023). Their mode of action is usually dose-dependent, redundant, orientation-independent, acting through binding of tissue-specific transcription factors and controlling tissue-specific gene expression (Will et al. 2017; Bordeira-Carriço et al. 2022). Enhancer-promoter communication may occur within large genomic distances, which are brought in close spatial proximity upon 3D-chromatin folding

(Bonev and Cavalli 2016; Furlong and Levine 2018). Topologically associating domains (TADs) are the functional units of 3D-chromatin architecture, restricting enhancers' interaction with their target promoters (Rao et al. 2014; Dixon et al. 2016). CNVs affecting TADs' structure by affecting the boundary between two separated TADs may trigger gene misexpression patterns and cause disease (Franke et al. 2016; Lupiáñez et al. 2016). Assigning function and pathogenicity to noncoding variants found in enhancers and other REs, in the next-generation sequencing era, remains challenging. The integration of multiple omics technologies and functional models is essential to elucidate the impact of RE perturbation and to establish a link to disease predisposition. Herein, we aim to identify and characterize novel HDGC-causing mechanisms involving REs regulating *CDH1* expression to solve the missing heritability in HDGC-like families, resourcing to WGS, chromatin analysis technologies and functional assays in cells and mice.

## Materials and Methods

*Patient selection*

Twenty-one patients from 19 HDGC-like families from various genetic backgrounds were admitted to BC Cancer in British Columbia, Canada and fulfilled the 1999 HDGC clinical criteria (Caldas et al. 1999). Families were re-classified according to (Blair et al. 2020) and HDGC-like families were considered if fulfilled criteria 1 and 2. Gastric cancers with diffuse component, with or without an intestinal component (mixed-type MGC) were considered for criteria 1. All patients tested negative for *CDH1* SNVs and CNVs. The present project was approved by the Ethical Committee of Centro Hospitalar Universitário de São João, with internal references 445-20 and 305-19.

*Whole genome sequencing*

Genomic DNA extracted from peripheral blood of 21 patients was sequenced using Illumina platform. Sequencing reads were mapped to the human reference genome (GRCh38) using BWA mem (v.0.7.15). Duplicated reads were marked, and their base quality score was recalibrated with GATK (v4.1.9.0, HTSJDK 2.23.0 and Picard 2.23.3).

*Variant calling*

SNVs were called with GATK – HaplotypeCaller tool (v4.1.9.0, HTSJDK 2.23.0 and Picard 2.23.3), and Depp Variant (Docker image: 1.3.0) (Poplin et al. 2018). Called SNVs were filtered according to quality control metrics, read depth (≥8) and genotype quality (≥20), and annotated with VEP (v.107). SNVs were prioritized if called by (1) both callers, from which HaplotypeCaller had high quality (≥200), (2A) Depp Variant, or (2B) HaplotypeCaller with extremely high quality (≥500). CNVs calling was performed with LUMPY (v 0.2.13) (Rausch et al. 2012; Layer et al. 2014), DELLY (v.0.9.1) and GRIDSS (v.2.13.2) (Cameron et al. 2017) , and annotated with AnnotSV (v. 2.5.2, Tcl (v. 8.6)) (Geoffroy et al. 2018). Structural variants with ≥1Mb length, inter-chromosomal events and variants lacking 'PASS' flag were discarded. CNVs were prioritized based on the following criteria: (Tier 1) called by LUMPY and DELLY with ≥90% overlap, and GRIDSS confirmed breakpoints with ≤4bp difference, (Tier 2A) called by DELLY and GRIDSS confirmed breakpoints with ≤4bp difference, (Tier 2B) called by LUMPY and GRIDSS confirmed breakpoints with ≤4bp difference, and (Tier 2C) LUMPY and DELLY with ≥90% overlap. Rare CNVs within the *CDH1* TAD (hg38: chr16: 68550001-69180000) were analysed to identify potential *CDH1* REs (AF<0.01). Rare coding CNVs and truncating SNVs in genes associated with gastrointestinal syndromes (AF<0.01; **Supplementary Table 1**) were assessed to exclude variants in other cancer-predisposing genes and further identify *CDH1* regulatory elements. For the polygenic approach, ultrarare deletions and truncating SNVs (AF<0.00001) observed in fewer than 6/21 patients (<24% of the cohort) were selected for analysis. Deletions in F4, F9 and F15 were validated by Sanger sequencing and SVs in F4 were validated by Pacbio sequencing as well.

*Chromatin availability data*

ATAC-seq (ENCSR337UIU, ENCSR970UNF) and ChIP-seq (ENCSR492BHN, ENCSR009RJD, ENCSR751BHO, ENCSR313DUH, ENCSR574USP, ENCSR078LIZ) data from normal stomach and colonic mucosa was collected from phase 3 ENCODE project (Abascal et al. 2020). GeneHancer enhancers and eQTLs were collected from the GeneHancer project (Fishilevich et al. 2017) and cCREs were collected from the ENCODE database (Moore et al. 2020).

*4C-seq*

Fresh gastric tissue from bariatric surgeries was collected and washed in HBSS 1x (Gibco). Gastric mucosa cells were scraped and enzymatically dissociated with collagenase type I (Merck), dispase (Merck), trypsin inhibitor (Sigma), BSA (Nzytech), dithiothreitol (Invitrogen) and HBSS 1x (Gibco) at 37ºC and 150rpm for at least 1h. 4C-seq libraries were generated, as previously described (van de Werken et al. 2012; Krijger et al. 2020), containing $1x10^7$ cells, cross-linked in 2% paraformaldehyde and lysed. Nuclei suspensions were digested with DnpII (New England Biolabs) as primary and Csp6I (New England Biolabs) as secondary restriction enzymes and re-circularized with T4 DNA Ligase (Thermo Fisher Scientific). 4C-seq libraries were purified using Amicon Ultra-15 10 kDa (MWCO) (Millipore) and PCR-amplified with 3.2µg per reaction (**supplementary table 2**). Samples were paired-end sequenced on Illumina HiSeqX technology (150bp reads) according to standard protocols. *CDH1* interactions on a genome scale were mapped from sequenced 4C libraries, using a bioinformatics pipeline based on Pipe4C (Krijger et al. 2020), PeakC for *cis* interactions (Geeven et al. 2018) with window size 2, alpha fdr 0.1 and minimal distance 500 and fourSig for *trans* interactions with window size 5, 1000 iterations, 0.001 fdr and 0.01 fdr probability and considered interactions in categories 1 and 2.

*Immunohistochemistry (IHC)*

Paraffin-embedded blocks containing adequate representation of the advanced tumour were selected for IHC testing. Parallel sections 5 µm thick were cut and stained with E-cadherin and *MLH1* (1:150; clone G168-728, BD Biosciences), or P-cadherin, using standard automated techniques. For each antibody, positive and negative external controls were placed on the same slide or on a separate control slide. Hematoxylin-eosin– and IHC-stained slides were analysed by two experienced pathologists.

*gDNA and RNA paraffin extraction*

Tumour/normal tissue was marked by an experienced pathologist and gDNA/RNA was extracted from six 10 µm thick slides. Tumour areas with at least 75% tumour cells were selected for extraction, using MagMax FFPE DNA/RNA Ultra Kit (Applied Biosystems, Life technologies), according to the manufacturer's instructions. Briefly, sections of paraffin-embedded tumour samples were de-paraffinized and protease K-digested. DNA and RNA

were bonded to magnetic beads, pelleted against a magnetic stand, and the supernatant containing DNA/RNA washed and eluted.

*Microsatellites instability analysis (MSI)*

Tumour tissue of the *MLH1* proband was studied for MSI using a panel of at least five dinucleotide repeat sequences, as described previously (Velho et al. 2008). Tumour was classified as 1) MSI-H if presented instability in ≥ 40% of the markers, 2) MSI-L if presented instability in <40% of the markers and 3) MSS if showed no instability in the tested markers.

*DNA Methylation Analysis*

gDNA extracted from tumour and normal counterpart were treated with bisulfite using Epitect Bisulfite kit (Qiagen). *MLH1* promoter was amplified by PCR using Multiplex PCR kit (Qiagen) and the primers depicted in **supplementary table 3**. PCR products were analysed in gel electrophoresis and Sanger sequenced on an ABI-3130 Genetic Analyzer (Applied Biosystems).

*Cell lines and culture conditions*

Human cell line MKN74 was purchased from the JCRB Cell Bank. MKN74 cell line and isogenic clones were cultured in RPMI medium (Gibco) supplemented with 10% foetal bovine serum (Biowest) and 1% Penicillin-Streptomycin (Gibco). HEK293T was cultured in DMEM medium supplemented with 10% foetal bovine serum (Biowest) and 1% Penicillin-Streptomycin (Gibco). Cells were maintained at 37ºC and 5% $CO_2$ in a high humidity atmosphere. Cell identification was confirmed by STR analysis and cells were confirmed to be free of mycoplasma contamination.

*In vitro functional assay by CRISPR-Cas9*

To test enhancer function, each region was targeted with CRISPR-Cas9. sgRNAs were designed using Benchling online platform (**supplementary table 3**). Individual sgRNAs (Invitrogen) were cloned in LentiCRISPRv2GFP (addgene 82416) or LentiCRISPRv2-mCherry (addgene 99154) vectors using BsmBIv2 (New England Biolabs). Plasmids were transformed into Stbl3 competent cells and colonies were sequenced (**supplementary table 3**). Lentiviral particles were produced resourcing to HEK293T cell line with pMD2.G (addgene 12259) and pCMV-dR8.91 (addgene) vectors, following Lipofectamine 3000 manufacture's protocol (Invitrogen) and collected at 48h. MKN74 was infected with pairs of lentivirus particles in medium supplemented with 10µg/µl hexadimethrine bromide (Merck Life Science S.L.U.) for 48h. Transduced cells were selected for GFP and mCherry positive expression at 7 days post-infection using FACS ARIA (BD Biosciences).

*Genotyping of edited clones*

gDNA was extracted using NZY Tissue gDNA isolation kit (NZYTech), according to the manufacturers' protocol. gDNA was amplified using primers flanking the edition sites (**supplementary table 3**) and Multiplex PCR kit (Qiagen). PCR products were analysed in gel electrophoresis and Sanger sequenced on an ABI-3130 Genetic Analyzer (Applied Biosystems).

*CDH1/E-cadherin and CDH3/P-cadherin expression analysis*

*CDH1*/*3* and *MLH1* mRNA expression was assessed by qPCR in triplicates for the MKN74 isogenic clones and in a single experiment for tumour/normal tissues from probands. RNA was extracted using mirVana RNA Isolation Kit (Invitrogen), according to manufacturers' protocol. cDNA was synthesized using SuperScriptII reverse transcriptase (Invitrogen), according to the manufacturers' protocol. mRNA expression was analyzed by qPCR with KAPA PROBE FAST qPCR Master Mix (2X) Kit (Sigma-Aldrich) and probes for *CDH1* (Hs.PT.58.3324071, TaqMan), *CDH3* (Hs.PT.51.5028751, IDT), *MLH1* (custom assay, IDT) and 18S (custom assay, IDT). Reactions were sequenced on a 7500 Real-Time PCR System (Applied Biosystems). Relative expression was normalized for the endogenous 18S control and quantified using the $2^{-\Delta\Delta Ct}$ method.

E-cadherin, P-cadherin and *MLH1* expression was assessed by flow cytometry in triplicates. Cells were detached with Versene (Gibco) and blocked with 3% bovine serum albumin-phosphatase buffer saline (Gibco). Cells were incubated with primary mouse monoclonal antibody HECD-1, P-cadherin or *MLH1* (1:100 dilution; 1h at 4ºC; Invitrogen), washed and incubated with secondary antibody anti-mouse Alexa Fluor 647 (Invitrogen). Fluorescence was measured using FACS Fortessa or Canto II (BD Biosciences) and Flow Jo version 10 software was used to analyse the data.

*Statistical analysis*

Statistical analysis was performed using GraphPad Prism version 7.00 software (GraphPad Software Inc.). A t-student test was used for comparison analysis, assuming equal variance between clones and parental samples. Differences were considered significant when p-value<0.05.

*Enhancer-reporter assays in vivo*

Enhancer activity was analyzed in transgenic mouse embryos using a site-specific integration protocol adapted for mouse embryonic stem cells (mESCs), as described previously (Phan et al. 2024). Briefly, the PhiC31 system (Chi et al. 2019) facilitated precise recombination between two att sites: an attP site inserted in a landing pad at the H11 safe-harbor genomic locus and an attB site within a donor vector containing the candidate enhancer and a puromycin selection marker (Sigma-Aldrich, P8833).

First, a mESC line was generated by CRISPR/Cas9 (FuGENE technology, Promega) to insert the H11 landing pad, which contained the Hsp68 promoter upstream of the LacZ

reporter gene (Hsp68::LacZ). This cell line served as a negative control to assess background staining. Candidate enhancer regions were PCR-amplified from human genomic DNA using PrimeSTAR GXL DNA Polymerase (Takara Bio) and primers with appropriate overhangs (**supplementary table 4**). Donor vectors were cloned by Gibson assembly (New England Biolabs; (Gibson et al. 2009)).

Subsequently, each donor plasmid was co-transfected with a PhiC31 plasmid into the Hsp68::LacZ mESC line using Lipofectamine LTX (Invitrogen). Transfected cells were selected with puromycin, and genetically modified mESCs were used to generate transgenic embryos via morula aggregation (Artus and Hadjantonakis 2011). CD1 female mice served as foster mothers.

At embryonic day E14.5, the embryos were harvested and processed for beta-galactosidase activity. Embryonic tissues were dissected in iced-cold 1X PBS, fixed in 4% paraformaldehyde (PFA) for 10 minutes and stained in beta-galactosidase solution at 37°C for a several hours to overnight, following Lobe et al. (1999). Dissected organs were imaged using a ZEISS SteREO Discovery.V12 microscope with a cold light source CL9000 and a Leica DFC420 digital camera (Leica Microsystems). Embryos were stored in 4% PFA in 1x PBS at 4°C.

## Results

We whole genome sequenced blood gDNA from 21 HDGC-like patients. Description of the cohort is depicted in **supplementary figure 1**. Following variant calling, we prioritized rare SNV, CNV and SV (AF<0.01), based on low frequency in cancer-free individuals in the *CDH1* TAD and in cancer syndrome-associated genes (**supplementary table 1**), and ultrarare deletions and truncating SNVs (AF<0.00001) that were common in our cohort (<6 patients, <24%).

*Variants within REs in the CDH1 TAD solve missing heritability in two HDGC families*

We identified potential REs within the *CDH1* TAD by extracting biochemical and chromatin annotations, such as histone modifications from ChIP-seq data in normal stomach. These marks were overlapped with regions that physically interact with the *CDH1* promoter in the same tissue, obtained through 4C-seq, and that display accessible chromatin identified through ATAC-seq. The list of potential REs was then crossed with CNVs and SVs found in HDGC families through WGS. We found a heterozygous deletion encompassing *CDH3* (encoding the P-cadherin protein) exons 1 and 2, intron 1 and part of intron 2, as well as two inversions (SVs) overlapping each side of the deletion boundaries in the proband of family F4 (**figure 1A,B**). These structural variants, validated by Pacbio long-read sequencing and Sanger sequencing, revealed a 20kb-deleted allele (a), and two inversions flanking the deletion, retaining most of the deleted sequence (b). However, the 5' and 3' breakpoints of this allele were not determined (b) (**figure 1B**). In addition, we found evidence for a wild-type sequence including the deleted region with non-inverted flanking regions (c) (**figure 1B**).

We focused on the *CDH3*-CNV impact in *CDH1* expression, by CRISPR-Cas9 deleting the *CDH3* 20kb sequence in a stomach-derived cell line. The homozygous deletion of this region led to complete loss of *CDH1* mRNA and E-cadherin protein (**figure 1C**), similar to a *CDH1* coding deletion (São José et al. 2023b). The homozygous *CDH3*-CNV also triggered complete loss of *CDH3*/P-cadherin expression (**supplementary figure 3 A, B**), as the deleted sequence includes the *CDH3* promoter, exon 1 and exon 2 (**figure 1A**). The tumour from family F4 proband presented mixed-type histology with signet ring cells, characteristic of HDGC tumours, and E-cadherin expression loss (**figure 1D, E**). Altogether, these results suggest that *CDH1* expression is regulated by REs lying within the *CDH3* 20kb deleted sequence.

As dramatic expression changes often depend on multiple REs being perturbed, we looked for REs within the 20kb deleted region. We found two potential *CDH1* REs within the deletion, namely a sequence interacting with the *CDH1* promoter in normal stomach epithelia found by 4C-seq, that displays accessible chromatin in a gastric cell line with normal *CDH1* expression (RE1), and a second sequence encompassing a *CDH1*-controlling expression quantitative trait loci (eQTL, RE2) (Fishilevich et al. 2017) (**figure 1B**). CRISPR-Cas9 homozygous deletion of RE1 alone led to 60% expression loss in *CDH1* mRNA and E-cadherin protein levels, while RE2 homozygous deletion alone caused 40% expression loss in *CDH1* mRNA and E-cadherin protein levels. The sum of the perturbation of RE1 and

342 RE2 independently, mimicked the impact of deleting the complete 20kb sequence (**figure**
343 **1C**). Deletion of the intronic RE1 did not interfere with *CDH3* mRNA nor with P-cadherin
344 protein expression, while deletion of the intronic RE2 led to 30% expression loss in *CDH3*/P-
345 cadherin (**supplementary figure 3 A,B**). These data suggest that RE2 modulated both
346 *CDH1* and *CDH3* expression, while RE1 modulated *CDH1* expression only. Enhancer
347 reporter assays in mouse embryos revealed strong enhancer activity in the forebrain for RE1
348 and RE2 sequences (**figure 1F**). While RE1 showed strong enhancer activity in the closing
349 palate, teeth, whiskers and eye, RE2 had mild activity in the stomach (**figure 1F**), correlating
350 well with tissues known to express *CDH1* during development (Stemmler et al. 2003).
351 Inversion of the 20Kb deleted region in F4, does not impact *CDH1* expression (*data not*
352 *shown*). As for the allele bearing the two inversions, the 5'-inversion places *CDH3* exon 2
353 ahead of exon 1 and part of the promoter, which is predicted to disrupt *CDH3* transcription
354 and translation initiation. A similar effect is expected for the 3'-inversion that inverts the
355 region spanning exon 3-8. The impact of these inversions in *CDH1* expression was not
356 assessed, yet the *CDH3*-CNV correlates well with *CDH1* expression loss and HDGC-related
357 phenotypes observed in family F4.

358 The tumour spectrum of Family F4 is broad, enclosing three gastric cancers (ages <40s), a
359 central nervous system tumour (age 40s), an ovarian cancer (age 20s), a skin cancer (age
360 50s) and a breast cancer (**figure 2A**). This young age of onset and broader tumour spectrum
361 may derive from the combined perturbation of *CDH1* and *CDH3*, impacting tissues beyond
362 the classically associated with *CDH1* impairment, and the activity of the deleted REs in
363 different tissues, as illustrated by the strong forebrain enhancer activity found in mice and
364 the presence of a central nervous system tumour (**figure 1F, 2A**).

365 We found that family F9, presenting with four gastric cancers (one in age 40s and three in
366 age 60s), three of which after age 60, and one colorectal cancer in 50s (**figure 2B**), carried
367 a 40bp deletion within the *CDH1-TANGO6* intergenic region, bearing *CDH1*-promotor
368 interactions in normal stomach (**figure 1A, B**). Homozygous deletion of the entire *CDH1-*
369 *TANGO6* intergenic region led to 50% reduction loss in *CDH1* mRNA and E-cadherin protein
370 levels (**figure 1C**). The deleted region showed enhancer activity in mouse embryos
371 forebrain, but not in the stomach or colon (**figure 1F**). Given that, in homozygosity, this
372 deletion triggers half *CDH1* expression loss, a third event may be required for gastric cancer
373 (GC) development, which can explain the latter age of cancer onset seen in this family.

374 Altogether, we reveal a novel mechanism impacting *CDH1* expression, through the
375 impairment of hypomorphic and dose-dependent enhancers within the *CDH1* TAD, likely
376 explaining cancer predisposition in two HDGC-like families.

377

378

379 *A variant within a long-distance stomach-specific RE solves missing heritability in one HDGC*
380 *family*

381 To further solve the missing heritability in the remaining HDGC-like families, we inquired the
382 WGS data from the remaining HDGC-like patients for rare (AF<0.01) SNVs, CNVs and SVs
383 in cancer syndrome-associated genes depicted in **supplementary table 1**. We found a

384 2.787-bp deletion encompassing the *MLH1* out-of-frame exon 13 and part of introns 12 and
385 13 in family F15 (**figure 3A**). *MLH1* is a Lynch syndrome mismatch repair gene associated
386 with Lynch syndrome, and its loss in cancer cells leads to microsatellite instability (MSI).
387 Indeed, the F15 proband's tumour showed *MLH1* expression loss, MSI and lacked *MLH1*
388 promoter methylation (**Figure 3B-D, supplementary figure 3 E**), arguing towards the
389 causality of the *MLH1*-CNV in HDGC predisposition in this family.

390 This family presents a proband with gastric carcinoma with lymphoid stroma and an evident
391 diffuse component at age 40s, and another two early-onset GCs (ages 30s and 40s) in a
392 sibling and their mother, suggesting variant segregation with disease through the maternal
393 side (**figure 3E**). GC preponderance and lack of colorectal cancers in this family was
394 unexpected, and raised the hypothesis that stomach-specific REs may reside within the
395 deleted region. Indeed, the *MLH1* deletion overlaps H3K4me1 peaks, chromatin marks of
396 active enhancers (RE3), that are present in normal stomach, but not in normal colon
397 epithelia (**figure 3F**). RE3 lacks H3K4me3 promoter chromatin marks in both stomach and
398 colon (**figure 3F**), suggesting this element may act as an enhancer, rather than a promoter.
399 We resorted to 4C-seq data from normal stomach epithelia and found evidence for a long-
400 distance interaction between *CDH1* and *MLH1* promoters (**figure 3F**), which could indicate
401 cross-regulation between these two genes. Supporting that the *MLH1* stomach-specific RE
402 could modulate *CDH1* expression, was the finding that E-cadherin was lost or mislocalized
403 in the diffuse component of the proband's tumour (**figure 3G, H**) and that *CDH1* mRNA was
404 reduced by 80% (**figure 3I**). A CRISPR/Cas9 clone mimicking the *MLH1* heterozygous CNV
405 triggered a reduction of 50% in the *MLH1* mRNA and protein expression levels
406 (**supplementary figure 3 C,D**), and of 40% in the *CDH1* mRNA and protein expression
407 levels (**figure 3J, K**).

408 Altogether, our results pinpoint an additional molecular mechanism, involving the germline
409 perturbation of stomach-specific REs at the *MLH1* locus, driving somatic *CDH1*/E-cadherin
410 downregulation and tumour MSI. This HDGC-like family may still be a Lynch syndrome
411 family with a particular tropism to the stomach, due to a deletion of a stomach-specific RE
412 with secondary impact in *CDH1* expression. Yet, the potential development of Lynch
413 syndrome-associated tumours may not be disregarded in the clinic.

414

415

416 *Multiple germline SNVs and CNV-deletions affecting stomach-specific regulatory elements*
417 *and immune-associated pathways occur in 50% of HDGC-like families*

418 We next explored the potential of a polygenic nature for the remaining HDGC families, by
419 evaluating the co-occurrence of variants across the genome. We searched the WGS data
420 for ultra-rare coding deletion-CNVs and truncating SNV (AF<0.00001), prioritized by at least
421 two callers, common in the cohort (≥6 patients, ≥24%) and absent in 13 controls from
422 1000genomes project. Overall, in 21 patients, we found 771 truncating SNVs and 11.860
423 CNVs, of which 1.547 were coding deletions. Each patient carried between 12 and 72 SNVs
424 and 22 and 209 CNVs. When combining all genes affected by the prioritized variants in
425 pathway analyses (**Figure 4A, supplementary figure 4**), we found a pathway-cluster that

426 was impacted in 10 HDGC-like patients mainly presenting DGC before age 50 (8/21) (**figure**
427 **4A, B, supplementary figure 4**). This cluster included immune-associated pathways,
428 encompassing antigen-presenting through major histocompatibility complex (MHC) class I,
429 natural killer, tumour cell killing and T cell mediated immunity (**figure 4A, B, supplementary**
430 **figure 4**). These pathways were not called for most families when considering SNVs alone,
431 but remained represented when considering CNV only (**supplementary figure 5**), which
432 are the main genetic event behind impairment of REs. We then asked whether deletions
433 overlapping stomach REs support GC predisposition. By focusing on deletions overlapping
434 accessible chromatin regions in normal stomach tissue by ATAC-seq, from 6.642 deletions,
435 415 overlapped accessible chromatin regions. Indeed, the same cluster of immune-
436 associated pathways seen in HDGC-like patients based on overall CNVs and SNVs, was
437 mimicked, despite the reduction in number of deletions overlapping stomach REs (**figure**
438 **4C, supplementary figure 6 A**). There were 39 genes recurrently impaired by deletions or
439 truncating SNVs, and five genes recurrently deleted in their regulatory sequence, in at least
440 three patients (**figure 6A**). We plotted these together with the monogenic events described
441 above in Figure 6, as well as the number of patients that presented immune-pathways
442 affected. Families F15 and F9, which presented germline *MLH1* and *CDH1-TANGO6*
443 intergenic CNVs, had no other genes impaired. Six probands and F19_3 family member
444 (invasive ductal breast cancer at age 50s) lacked variants in these pathways, mimicking the
445 controls. Besides the *CDH3* germline CNV and SVs, F4 also displayed impaired immune-
446 associated genes/pathways. The remaining nine probands and additional member of F19
447 (F19_1 with intestinal GC at 30s, F19_2 with DGC at 60s) presented between 3 and 27
448 deleted genes (**figure 6A**). Additionally, from 10 probands with impaired germline landscape
449 in immune-related genes, eight had age of onset below 50 years of age (mean age of onset:
450 47,2 years±16,8) (**figure 6B**). While 7 individuals with deletions overlapping stomach REs
451 had age of onset below 50 (mean age of onset: 38,4 years±8,5) from 12 individuals (**figure**
452 **6B**).

453

## Discussion

More than half of HDGC suspected families remain molecularly undiagnosed (HDGC-like), many of them displaying germline monoallelic *CDH1* downregulation and E-cadherin loss in the tumour (Pinheiro et al. 2010). These data pinpoint *CDH1* as the main gene triggering HDGC. Herein, we worked under the hypothesis that perturbation of REs controlling *CDH1* expression drive HDGC predisposition in HDGC-like families.

This study presents compelling evidence supporting the conclusion that cancer predisposition in 16% (3/19) of HDGC-like families within our cohort is explained by alterations occurring in the *CDH1* regulatory network, within and beyond the *CDH1* TAD. Importantly, the high frequency of HDGC-like families (10/19 – 53%) bearing ultra-rare deletions overlapping stomach REs and impairing immune-associated pathways, calls for a multigenic regulatory landscape contributing to HDGC predisposition.

The *CDH1* TAD is expected to be the most enriched region of the genome in REs modulating the *CDH1* locus (Zuin et al. 2022). Within the *CDH1* TAD, enclosing eight genes and a total of 630kb, we found a *CDH3* 20-kb deletion encompassing two noncoding hypomorphic and dose-dependent enhancers controlling *CDH1* expression, which likely represent a novel biological mechanism of HDGC predisposition in family F4. The *CDH1*/E-cadherin loss in the diffuse component of the tumour further argues towards the role of this deletion in HDGC predisposition. The combined deletion of two *CDH1* enhancers, each contributing to half *CDH1* expression loss, represents a classical mechanism of enhancer-driven expression control in *CDH1*-expressing tissues (Stemmler et al. 2005; Will et al. 2017). In this family, this heterozygous *CDH3*-CNV produces an expression loss similar to that induced by a heterozygous coding truncating *CDH1* variants and is expected to lead to germline *CDH1* monoallelic expression, which would explain the occurrence of GC with a diffuse component in the proband, her brother and mother. Indeed, CD44-Cre/*Cdh1*$^{fl/fl}$ mice develop stage 1 mixed-type gastric cancer (Decourtye-Espiard and Guilford 2023), correlating well with a tumour with mixed-type histology reduced *CDH1* expression. Although we could not assess the impact of the *CDH3* inversions, likely inherited from the paternal side, these are more likely to impact *CDH3* expression rather than *CDH1* expression, as the enhancers are orientation-independent. In fact, we found that inversion of the 20kb deleted region in F4, does not impact *CDH1* expression (*data not shown*). The compound heterozygous state found for *CDH3* (allele 1: deletion + allele 2: inversions) in F4 proband, leading to nearly complete loss of *CDH3* expression, supports the tumour spectrum found in this family, which goes beyond the classical HDGC disease spectrum (Garcia-Pelaez et al. 2023). In contrast to normal stomach epithelia, which does not express *CDH3*, ovary and skin do (Cao et al. 2020), which may explain why biallelic loss of *CDH3* may predispose to the ovarian and skin tumours observed in the family. Even if only one of the *CDH3* alleles has been inherited by other affected family members, it may still cause cancer predisposition, as combined loss of function occurs for both *CDH1* and *CDH3* (allele 1: deletion) with a single allele being targeted. Furthermore, the central nervous system tumour occurrence correlates well with the forebrain enhancer activity observed for the RE1 and RE2 contained within the *CDH3*-CNV. *CDH3* loss of expression through combined deletion of the *CDH3* promoter, exon 1 and 2, and/or an inversion of the 5'-region of *CDH3* may also trigger ectodermal dysplasia,

497 ectrodactyly and macular dystrophy syndrome or congenital hypotrichosis with juvenile
498 macular dystrophy syndrome, both autosomal recessive (OMIM ID 601553). However, as
499 far as we know, these diseases have not been reported for this family.

500 The *CDH1-TANGO6* intergenic sequence also encompasses a noncoding hypomorphic
501 enhancer, but homozygous deletion triggers loss of only half *CDH1* expression. In addition,
502 the mean cancer age of onset in family F9 (63.7 years of age) is higher than what is usually
503 found for HDGC families (42±12,16 years of age) (Garcia-Pelaez et al. 2023). Taken
504 together, a third inactivation event may be required for GC development in F9 carriers, which
505 would take more time to occur. This 3-hit hypothesis would in part explain the later cancer
506 onset in this family. Deletion of this intergenic region in combination with a 3'-coding deletion
507 of the *CDH1* has been shown to trigger extremely early GC onset and high disease
508 penetrance (São José et al. 2023a). That deletion, in contrast to the current one, strongly
509 reduced *CDH1* expression and led to re-wiring of the 3D chromatin structure, impairing the
510 transcriptome, immune, proliferation and adhesion-associated pathways, as compared to a
511 deletion of *CDH1* alone (São José et al. 2023a). Thus, we propose that deletion of REs lying
512 in the *CDH1-TANGO6* intergenic sequence occurring in both families, modulates *CDH1*
513 expression and predisposes carriers to GC development. This likely occurs later in life in F9,
514 because the *CDH1* coding region remains wild-type (São José et al. 2023a).

515 In a knowledge-driven approach, we next explored rare CNVs and SNVs in cancer-
516 syndrome-associated genes and found a germline *MLH1* deletion, that has not been
517 previously identified in Lynch syndrome families to date, according to the InSiGHT database.
518 Although *MLH1* loss of function predisposes individuals to Lynch syndrome, preferentially
519 increasing the risk of colorectal and endometrial cancers, intestinal-type GC may also occur,
520 with an estimated risk of 13% at age 80 (Møller et al. 2018). In family F15, the clinical history
521 is restricted to GC, but the proband's tumour presents not only diffuse, but also intestinal
522 histology, which is consistent with *MLH1* expression loss and MSI (Møller et al. 2018).
523 Further supporting the hypothesis that GC predisposition is associated with *MLH1* in this
524 family, somatic *MLH1* promoter methylation, a hallmark of MSI in sporadic colorectal and
525 GCs, was negative in the proband's tumour (Shen et al. 2018). Our data raised the
526 hypothesis that *CDH1* expression disruption was involved not only in generating the diffuse
527 component of this tumour, but also in shifting the *MLH1*-related tumour spectrum to the
528 stomach. Indeed, not only were *CDH1*/E-cadherin mRNA and protein found to be
529 downregulated in the tumour, but also the deleted sequence encompassed enhancer
530 chromatin marks present in normal stomach tissue and absent from normal colon mucosa.
531 Also, an interaction found by 4C-seq between *CDH1* and *MLH1* promoters further supported
532 a cross-regulation between both genes. Rare inter-chromosomal interactions have been
533 observed among neighbouring chromosomal territories, such as CISTR-ACT in
534 chromosome 12 and SOX9 in chromosome 17 (Quinodoz et al. 2018; Milad Mokhtaridoost
535 et al. 2024). Altogether, these data indicate that the *MLH1* exon 13 sequence, and its intronic
536 vicinity, act as a tissue-specific RE, controlling the expression of *CDH1*, specifically in the
537 stomach. This regulatory module and the loss of *MLH1* expression, as a consequence of
538 deleting an out-of-frame exon, would concomitantly trigger MSI in the emerging GCs. To our

539 knowledge, this is the first report associating a *MLH1* exon 13 deletion with *CDH1* loss, and
540 its associated stomach-specific REs with GC predisposition.

541 The novel genetic alterations described above, as potential causes for three HDGC-like
542 families, do not affect the structure of the *CDH1* locus, but rather involve *CDH1* enhancers
543 located either within the *CDH1* TAD or located in another chromosome. In all instances, the
544 downregulation of *CDH1* occurs due to transcriptional impairment caused by deletion of
545 enhancers for which long distance interactions have been identified herein. Similar
546 mechanisms have been described for several genes predisposing to developmental
547 disorders (Will et al. 2017).

548 It is also worth mentioning that probands from HDGC-like families F4 (*CDH3* CNVs and
549 SVs) and F15 (*MLH1* CNV) present mixed GC with a diffuse component, rather than pure
550 DGC, which suggests that impairment of *CDH1* REs outside of the *CDH1* locus may have
551 wider impacts than the impairment of the *CDH1* locus alone. This becomes evident not only
552 in the different histology of GCs, but also in the diversity of cancers in family F4.

553 Given the lack of obvious variants in the remaining 16 families, we explored the germline
554 regulatory landscape of HDGC undiagnosed families. The germline regulatory landscape of
555 undiagnosed families encompasses mainly downregulation of immune-associated
556 pathways. A specific cluster was found for younger affected individuals, with downregulation
557 of pathways associated with MHC I and natural killer immunity, absent in healthy controls,
558 which are known to play a role in GC immune evasion (Shen et al. 2005; Na et al. 2021).
559 Interestingly, earlier onset DGC patients display a higher number of deletions in genome-
560 wide open chromatin regions in normal stomach tissue, compared to patients with older
561 cancer onset. These "younger-onset"-related regions encompass immune-affected
562 pathways, recapitulating the germline regulatory landscape and pinpointing stomach REs
563 as possible genetic drivers. Altogether, the observed immune impairment in HDGC families
564 may result in lower immunological surveillance in early stages of intramucosal signet-ring
565 cell carcinoma *foci*, characteristic of HDGC tumours. Indeed, variants in immune
566 surveillance genes, such as MHC class I, have been suggested to play a role in intramucosal
567 signet-ring cell carcinoma *foci* (Decourtye-Espiard and Guilford 2023), yet their
568 consolidation is requires additional research. Interestingly, families F15 and F9 lack
569 additional alterations to the *MLH1* CNV and the *CDH1-TANGO6* intergenic CNVs,
570 suggesting these were sufficient to trigger the HDGC phenotypes. Indeed, F15 (*MLH1* CNV)
571 tumour presents high degree of inflammation, highlighting that the lack of germline defects
572 in immune-related pathways allows the immune system to recognize tumor cells. In this
573 particular case, the F15 proband would benefit from immunotherapy treatment (Chao et al.
574 2021). In contrast, family F4 displays impaired immune-associated genes/pathways as well
575 as the *CDH3* CNV and SVs.

576 Immune-associated genes and several mucins were also found impaired in other HDGC-
577 like families. Supporting the role of *MUC4* in this context is the reduced expression described
578 in poorly differentiated GC or signet-ring cell carcinoma (Tamura et al. 2012), also
579 characteristic of HDGC (Carneiro et al. 1995; van der Post et al. 2016). Downregulation of
580 the stomach-specific *MUC6* gene (Babu et al. 2006) was found to be associated with
581 advanced stages of GC and poor prognosis (Shi and Xi 2021), supporting an association

582 with HDGC. Indeed, homozygous deletion of *MUC6* causes spontaneous GC development
583 with accumulation of $CD45^+$ T-cells in normal and tumour tissue (Arai et al. 2024).
584 Impairment of T-cell regulatory mechanisms and MHC-related immune surveillance in the
585 germline with co-occurrence of mucins reduced expression may pinpoint a polygenic
586 mechanism for GC development in HDGC families.

587 Altogether, impairment of immune- and mucins-associated pathways/genes may constitute
588 a germline genetic background capable of regulating HDGC development in the presence
589 of a primary unknown triggering mechanism.

590 Taken together, our data resolves the missing heritability in 3 out of 19 HDGC undiagnosed
591 families, corresponding to 16% of the entire cohort, and pinpointed novel mechanisms of
592 HDGC predisposition related with *CDH1* REs as regulators of *CDH1*/E-cadherin expression.
593 The finding of a causal mechanism promotes re-engagement with the family, genetic
594 counselling and disease risk management of individuals at risk. The germline landscape of
595 younger DGC patients includes downregulation of immune-associated pathways and
596 several mucins, which may play a role in immune surveillance and DGC development when
597 triggered by a still unknown mechanism.

598

599

## Acknowledgments

This work received funding from: (1) the European Union's Horizon 2020 research and innovation programme under grant agreement No 779257 (Solve-RD: H2020-SC1-2017-Single-Stage-RTD), which provided Ph.D. salaries to JG-P; (2) The European Regional Development Fund (ERDF) through the COMPETE 2020-Operacional Programme for Competitiveness and Internationalisation (POCI), Portugal 2020, and by Portuguese funds through Fundacao para a Ciencia e Tecnologia (FCT)/Ministerio da Ciencia, Tecnologia e Inovação (3DChroMe: PTDC/BTM-TEC/30164/2017, LEGOH: PTDC/BTM-TEC/6706/2020, DGCoding: 2023.11994.PEX); (3) FCT with salary support for PhD studentships to CSJ (Ref. SFRH/BD/140796/2018), MF (Ref. 2020.05763.BD) and SL (Ref. 2020.05773.BD). Further, this study has received funding from the European Union's Horizon Europe Coordination and Support action under the Grant Agreement nº 101095483 (PREVENTABLE). Views and opinions expressed are however those of the author(s) only and do not necessarily reflect those of the European Union or The Health and Digital Executive Agency (HaDEA). Neither the European Union nor the granting authority can be held responsible for them.

This work was supported by: (1) Doctoral Programme in Biomedicine - Faculty of Medicine, University of Porto, to CSJ and JG-P; (2) Doctoral Programme in Computational Sciences, Faculty of Sciences, University of Porto, to MF; (3) Doctoral Programme on Cellular and Molecular Biotechnology Applied to Health Sciences, School of Medicine and Biomedical Sciences, University of Porto, Portugal, to SL.

## Author Contributions

Carla Oliveira: supervision, Project administration, funding acquisition; Celina S. José and Carla Oliveira: conceptualization, formal analysis; José García-Pelaez, Janine Sanz, Lilian Cordova, Pardeep Kourah: acquisition of clinical and pathological data; Irene Gullo: pathological analysis; Celina S. José, Ana Pedro, Ana André, Silvana Lobo: *in vitro* experimental work; Marta Ferreira and Celina S. José: bioinformatic analysis; Celina S. José: integration of genetics, clinical and functional data; Celina S. José, Fiona Puntieri and Juliane Glaser: *in vivo* experimental work; All authors: writing, review, editing and approval of the manuscript.

## References

Abascal F, Acosta R, Addleman NJ, et al (2020) Expanded encyclopaedias of DNA elements in the human and mouse genomes. Nature 583:699–710. https://doi.org/10.1038/S41586-020-2493-4

Arai J, Hayakawa Y, Tateno H, et al (2024) The role of gastric mucins and mucin-related glycans in gastric cancers. Cancer Sci 115:2853–2861. https://doi.org/10.1111/cas.16282

Artus J, Hadjantonakis A-K (2011) Generation of chimeras by aggregation of embryonic stem cells with diploid or tetraploid mouse embryos. Methods Mol Biol 693:37–56. https://doi.org/10.1007/978-1-60761-974-1_3

Babu SD, Jayanthi V, Devaraj N, et al (2006) Expression profile of mucins (MUC2, MUC5AC and MUC6) in Helicobacter pylori infected pre-neoplastic and neoplastic human gastric epithelium. Mol Cancer 5:. https://doi.org/10.1186/1476-4598-5-10

Benusiglio PR, Colas C, Guillerm E, et al (2019) Clinical implications of CTNNA1 germline mutations in asymptomatic carriers. Gastric Cancer 22:899–903. https://doi.org/10.1007/s10120-018-00907-7

Blair VR, McLeod M, Carneiro F, et al (2020) Hereditary diffuse gastric cancer: updated clinical practice guidelines. Lancet Oncol 21:e386–e397. https://doi.org/10.1016/S1470-2045(20)30219-9

Bonev B, Cavalli G (2016) Organization and function of the 3D genome. Nat Rev Genet 17:661–678. https://doi.org/10.1038/NRG.2016.112

Bordeira-Carriço R, Teixeira J, Duque M, et al (2022) Multidimensional chromatin profiling of zebrafish pancreas to uncover and investigate disease-relevant enhancers. Nat Commun 13:1945. https://doi.org/10.1038/s41467-022-29551-7

Caldas C, Carneiro F, Lynch HT, et al (1999) Familial gastric cancer: overview and guidelines for management. J Med Genet 36:873–880

Cameron DL, Schröder J, Penington JS, et al (2017) GRIDSS: sensitive and specific genomic rearrangement detection using positional de Bruijn graph assembly. Genome Res 27:2050–2060. https://doi.org/10.1101/GR.222109.117

Cao J, O'Day DR, Pliner HA, et al (2020) A human cell atlas of fetal gene expression. Science 370:. https://doi.org/10.1126/SCIENCE.ABA7721

Carneiro F, Seixas M, Sobrinho-Simões M (1995) New elements for an updated classification of the carcinomas of the stomach. Pathol Res Pract 191:571–584. https://doi.org/10.1016/S0344-0338(11)80878-2

Chao J, Fuchs CS, Shitara K, et al (2021) Assessment of Pembrolizumab Therapy for the Treatment of Microsatellite Instability–High Gastric or Gastroesophageal Junction Cancer Among Patients in the KEYNOTE-059, KEYNOTE-061, and KEYNOTE-062 Clinical Trials. JAMA Oncol 7:895. https://doi.org/10.1001/jamaoncol.2021.0275

Chi X, Zheng Q, Jiang R, et al (2019) A system for site-specific integration of transgenes in mammalian cells. PLoS One 14:e0219842. https://doi.org/10.1371/journal.pone.0219842

Cova G, Glaser J, Schöpflin R, et al (2023) Combinatorial effects on gene expression at the Lbx1/Fgf8 locus resolve split-hand/foot malformation type 3. Nat Commun 14:. https://doi.org/10.1038/S41467-023-37057-Z

Decourtye-Espiard L, Guilford P (2023) Hereditary Diffuse Gastric Cancer. Gastroenterology 164:719–735. https://doi.org/10.1053/J.GASTRO.2023.01.038

Dixon JR, Gorkin DU, Ren B (2016) Chromatin Domains: The Unit of Chromosome Organization. Mol Cell 62:668–680. https://doi.org/10.1016/j.molcel.2016.05.018

Fishilevich S, Nudel R, Rappaport N, et al (2017) GeneHancer: genome-wide integration of enhancers and target genes in GeneCards. Database (Oxford) 2017:. https://doi.org/10.1093/database/bax028

Franke M, Ibrahim DM, Andrey G, et al (2016) Formation of new chromatin domains determines pathogenicity of genomic duplications. Nature 538:265–269. https://doi.org/10.1038/nature19800

Furlong EEM, Levine M (2018) Developmental enhancers and chromosome topology. Science (1979) 361:1341–1345. https://doi.org/10.1126/science.aau0320

Garcia-Pelaez J, Barbosa-Matos R, Lobo S, et al (2023) Genotype-first approach to identify associations between CDH1 germline variants and cancer phenotypes: a multicentre study by the European Reference Network on Genetic Tumour Risk Syndromes. Lancet Oncol 24:91–106. https://doi.org/10.1016/S1470-2045(22)00643-X

Geeven G, Teunissen H, de Laat W, de Wit E (2018) peakC: a flexible, non-parametric peak calling package for 4C and Capture-C data. Nucleic Acids Res 46:e91. https://doi.org/10.1093/nar/gky443

Geoffroy V, Herenger Y, Kress A, et al (2018) AnnotSV: an integrated tool for structural variations annotation. Bioinformatics 34:3572–3574. https://doi.org/10.1093/bioinformatics/bty304

Gibson DG, Young L, Chuang R-Y, et al (2009) Enzymatic assembly of DNA molecules up to several hundred kilobases. Nat Methods 6:343–345. https://doi.org/10.1038/nmeth.1318

Guilford P, Hopkins J, Harraway J, et al (1998) E-cadherin germline mutations in familial gastric cancer. Nature 392:402–405. https://doi.org/10.1038/32918

Gullo I, Grillo F, Mastracci L, et al (2020) Precancerous lesions of the stomach, gastric cancer and hereditary gastric cancer syndromes. Pathologica 112:166–185. https://doi.org/10.32074/1591-951X-166

Hansford S, Kaurah P, Li-Chang H, et al (2015) Hereditary Diffuse Gastric Cancer Syndrome: CDH1 Mutations and Beyond. JAMA Oncol 1:23–32. https://doi.org/10.1001/jamaoncol.2014.168

Krijger PHL, Geeven G, Bianchi V, et al (2020) 4C-seq from beginning to end: A detailed protocol for sample preparation and data analysis. Methods 170:17–32. https://doi.org/10.1016/J.YMETH.2019.07.014

Layer RM, Chiang C, Quinlan AR, Hall IM (2014) LUMPY: a probabilistic framework for structural variant discovery. Genome Biol 15:. https://doi.org/10.1186/GB-2014-15-6-R84

Lobe CG, Koop KE, Kreppner W, et al (1999) Z/AP, a double reporter for cre-mediated recombination. Dev Biol 208:281–292. https://doi.org/10.1006/dbio.1999.9209

Lobo S, Benusiglio PR, Coulet F, et al (2021) Cancer predisposition and germline CTNNA1 variants. Eur J Med Genet 64:104316. https://doi.org/10.1016/j.ejmg.2021.104316

Lupiáñez DG, Spielmann M, Mundlos S (2016) Breaking TADs: How Alterations of Chromatin Domains Result in Disease. Trends in Genetics 32:225–237. https://doi.org/10.1016/j.tig.2016.01.003

Majewski IJ, Kluijt I, Cats A, et al (2013) An α-E-catenin (CTNNA1) mutation in hereditary diffuse gastric cancer. J Pathol 229:621–629. https://doi.org/10.1002/path.4152

Milad Mokhtaridoost, Jordan J Chalmers, Marzieh Soleimanpoor, et al (2024) Inter-chromosomal contacts demarcate genome topology along a spatial gradient. Nat Commun 15(1):9813:

Møller P, Seppälä TT, Bernstein I, et al (2018) Cancer risk and survival in path_MMR carriers by gene and gender up to 75 years of age: a report from the Prospective Lynch Syndrome Database. Gut 67:1306–1316. https://doi.org/10.1136/GUTJNL-2017-314057

Moore JE, Purcaro MJ, Pratt HE, et al (2020) Expanded encyclopaedias of DNA elements in the human and mouse genomes. Nature 583:699–710. https://doi.org/10.1038/s41586-020-2493-4

Na HY, Park Y, Nam SK, et al (2021) Prognostic significance of natural killer cell-associated markers in gastric cancer: quantitative analysis using multiplex immunohistochemistry. J Transl Med 19:. https://doi.org/10.1186/S12967-021-03203-8

Oliveira C, Pinheiro H, Figueiredo J, et al (2015) Familial gastric cancer: genetic susceptibility, pathology, and implications for management. Lancet Oncol 16:e60-70. https://doi.org/10.1016/s1470-2045(14)71016-2

Oliveira C, Senz J, Kaurah P, et al (2009a) Germline CDH1 deletions in hereditary diffuse gastric cancer families. Hum Mol Genet 18:1545–1555. https://doi.org/10.1093/hmg/ddp046

Oliveira C, Seruca R, Carneiro F (2009b) Hereditary gastric cancer. Best Pract Res Clin Gastroenterol 23:147–157. https://doi.org/10.1016/j.bpg.2009.02.003

Oliveira C, Sousa S, Pinheiro H, et al (2009c) Quantification of epigenetic and genetic 2nd hits in CDH1 during hereditary diffuse gastric cancer syndrome progression. Gastroenterology 136:2137–2148. https://doi.org/10.1053/j.gastro.2009.02.065

Phan MH, Zehnder TM, Puntieri F, et al (2024) Conservation of Regulatory Elements with Highly Diverged Sequences Across Large Evolutionary Distances

Pinheiro H, Bordeira-Carrico R, Seixas S, et al (2010) Allele-specific CDH1 downregulation and hereditary diffuse gastric cancer. Hum Mol Genet 19:943–952. https://doi.org/10.1093/hmg/ddp537

Poplin R, Chang PC, Alexander D, et al (2018) A universal SNP and small-indel variant caller using deep neural networks. Nat Biotechnol 36:983. https://doi.org/10.1038/NBT.4235

Quinodoz SA, Ollikainen N, Tabak B, et al (2018) Higher-Order Inter-chromosomal Hubs Shape 3D Genome Organization in the Nucleus. Cell 174:744-757.e24. https://doi.org/10.1016/j.cell.2018.05.024

Rao SSP, Huntley MH, Durand NC, et al (2014) A 3D map of the human genome at kilobase resolution reveals principles of chromatin looping. Cell 159:1665–1680. https://doi.org/10.1016/J.CELL.2014.11.021

Rausch T, Zichner T, Schlattl A, et al (2012) DELLY: structural variant discovery by integrated paired-end and split-read analysis. Bioinformatics 28:. https://doi.org/10.1093/BIOINFORMATICS/BTS378

São José C, Garcia-Pelaez J, Ferreira M, et al (2023a) Combined loss of CDH1 and downstream regulatory sequences drive early-onset diffuse gastric cancer and increase penetrance of hereditary diffuse gastric cancer. Gastric Cancer. https://doi.org/10.1007/S10120-023-01395-0

São José C, Pereira C, Ferreira M, et al (2023b) 3D Chromatin Architecture Re-Wiring at the CDH3/CDH1 Loci Contributes to E-Cadherin to P-Cadherin Expression Switch in Gastric Cancer. Biology (Basel) 12:803. https://doi.org/10.3390/biology12060803

Shen S, Chen X, Li H, et al (2018) *MLH1* Promoter Methylation and Prediction/Prognosis of Gastric Cancer: A Systematic Review and Meta and Bioinformatic Analysis. J Cancer 9:1932–1942. https://doi.org/10.7150/jca.23284

Shen YQ, Zhang JQ, Miao FQ, et al (2005) Relationship between the downregulation of HLA class I antigen and clinicopathological significance in gastric cancer. World J Gastroenterol 11:3628–3631. https://doi.org/10.3748/WJG.V11.I23.3628

Shi D, Xi X (2021) Regulation of MUC6 Methylation Correlates with Progression of Gastric Cancer. Yonsei Med J 62:1005. https://doi.org/10.3349/ymj.2021.62.11.1005

Spielmann M, Lupiáñez DG, Mundlos S (2018) Structural variation in the 3D genome. Nat Rev Genet 19:453–467. https://doi.org/10.1038/S41576-018-0007-0

Stemmler MP, Hecht A, Kemler R (2005) E-cadherin intron 2 contains cis-regulatory elements essential for gene expression. Development 132:965–76. https://doi.org/10.1242/dev.01662

Stemmler MP, Hecht A, Kinzel B, Kemler R (2003) Analysis of regulatory elements of E-cadherin with reporter gene constructs in transgenic mouse embryos. Developmental Dynamics 227:238–245. https://doi.org/10.1002/dvdy.10301

Tamura Y, Higashi M, Kitamoto S, et al (2012) MUC4 and MUC1 expression in adenocarcinoma of the stomach correlates with vessel invasion and lymph node metastasis: an immunohistochemical study of early gastric cancer. PLoS One 7:. https://doi.org/10.1371/JOURNAL.PONE.0049251

Tedaldi G, Pirini F, Tebaldi M, et al (2019) Multigene Panel Testing Increases the Number of Loci Associated with Gastric Cancer Predisposition. Cancers (Basel) 11:. https://doi.org/10.3390/CANCERS11091340

van de Werken HJ, de Vree PJ, Splinter E, et al (2012) 4C technology: protocols and data analysis. Methods Enzymol 513:89–112. https://doi.org/10.1016/b978-0-12-391938-0.00004-5

van der Post RS, Gullo I, Oliveira C, et al (2016) Histopathological, Molecular, and Genetic Profile of Hereditary Diffuse Gastric Cancer: Current Knowledge and Challenges for the Future. Adv Exp Med Biol 908:371–391. https://doi.org/10.1007/978-3-319-41388-4_18

Velho S, Moutinho C, Cirnes L, et al (2008) BRAF, KRAS and PIK3CA mutations in colorectal serrated polyps and cancer: Primary or secondary genetic events in colorectal carcinogenesis? BMC Cancer 8:255. https://doi.org/10.1186/1471-2407-8-255

Will AJ, Cova G, Osterwalder M, et al (2017) Composition and dosage of a multipartite enhancer cluster control developmental expression of Ihh (Indian hedgehog). Nat Genet 49:1539–1545. https://doi.org/10.1038/ng.3939

Zuin J, Roth G, Zhan Y, et al (2022) Nonlinear control of transcription through enhancer–promoter interactions. Nature 604:571–577. https://doi.org/10.1038/s41586-022-04570-y

A

| Family | Gene | Syndrome | Location hg38 | SV size (bp) | SV type | Perturbed region | AF |
|---|---|---|---|---|---|---|---|
| F4 | *CDH3* | Cancer | chr16:68645346-68665730 | 20384 | DEL | Prom, exon1-2, intron 1-2 | novel |
| F4 | *CDH3* | Cancer | chr16:68616149-68647665 | 31516 | INV | Prom, exon1-2, intron 1-2 | novel |
| F4 | *CDH3* | Cancer | chr16:68663492-68680068 | 16576 | INV | Intron 2-7 exon 3-8 | novel |
| F9 | *CDH1-TANGO6* intergenic | - | chr16:68837494-68837533 | 39 | DEL | Intergenic | novel |

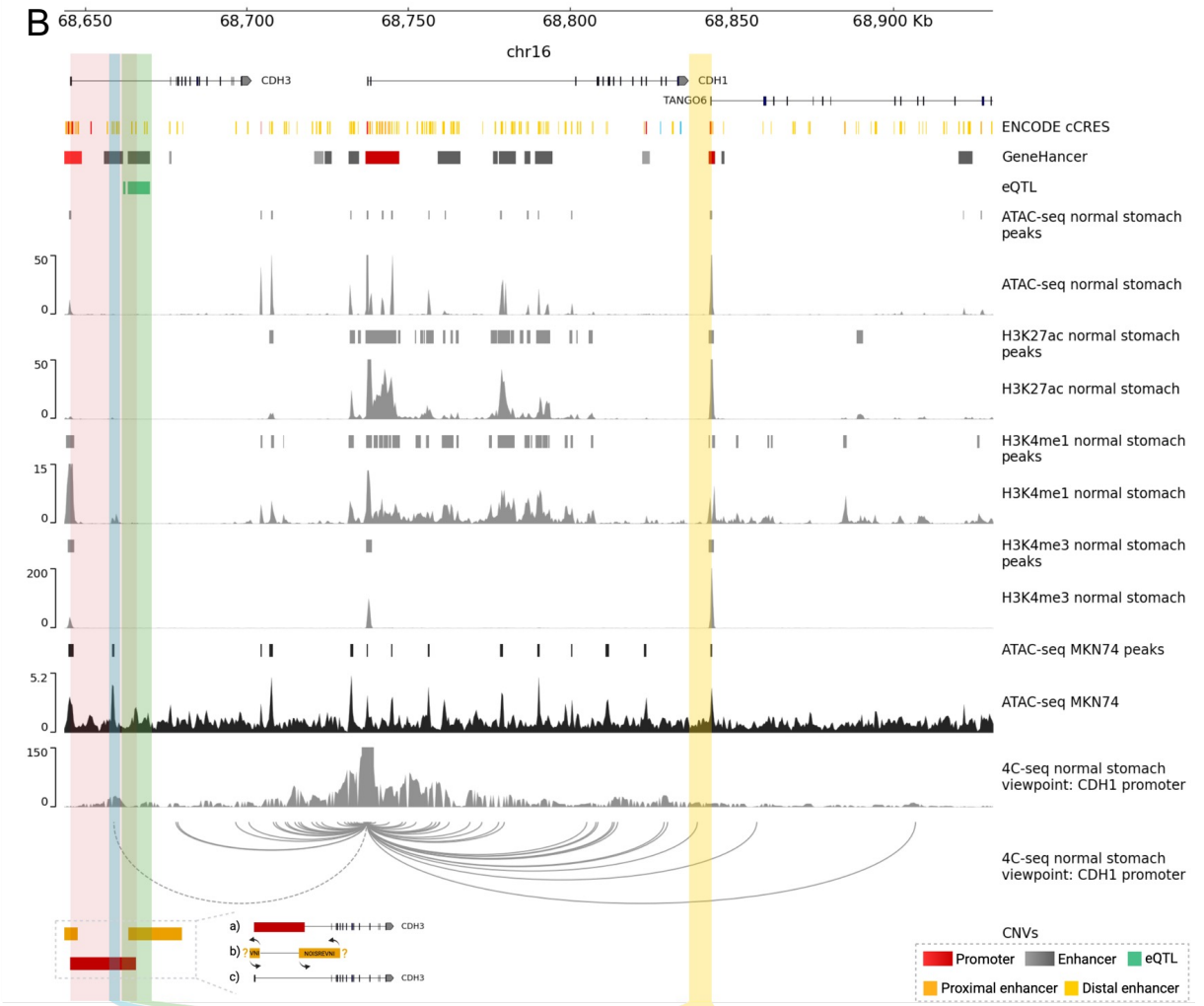


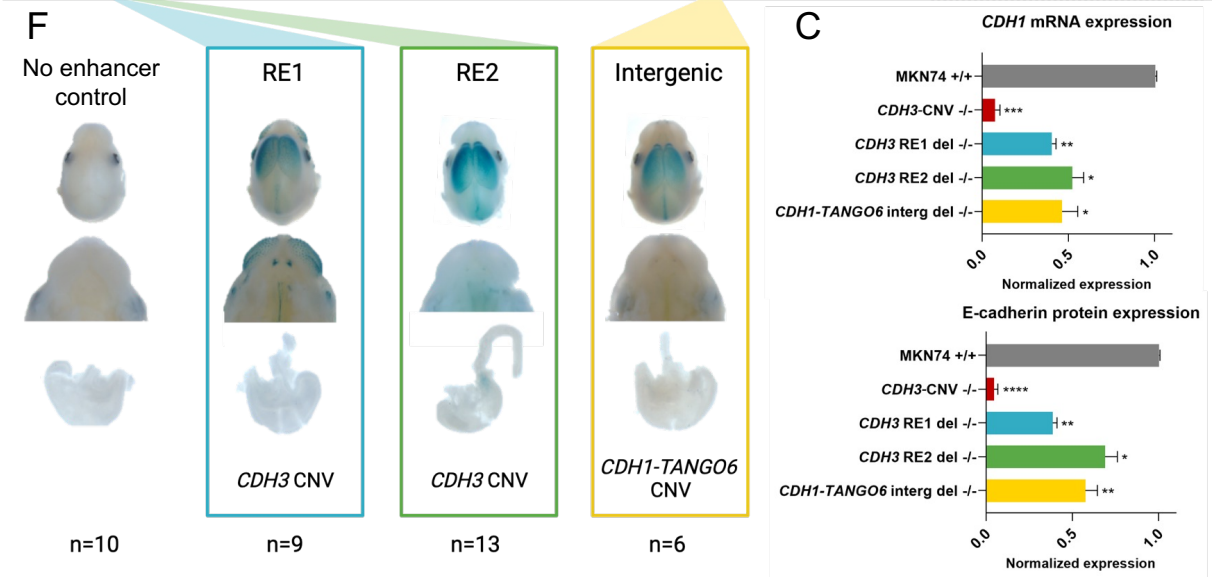





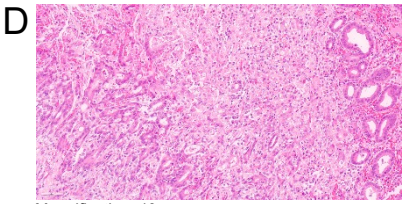


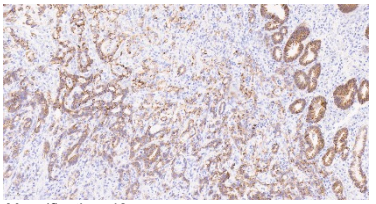


***Figure 1. Genomic CNVs in CDH1 TAD.*** *A) Description of identified CNVs, B) Candidate REs, chromatin marks, and CDH1 interactors in normal stomach tissue, C) CDH1 mRNA and protein expression of edited MKN74 clones, D) Hematoxylin and eosin of tumour tissue from proband with CDH3 CNV, E) E-cadherin expression of tumour tissue from proband with CDH3 CNV (immunohistochemistry), F) Enhancer assay of candidate REs in mouse embryos, blue precipitate represent β-galactosidase expression and tissue-specific enhancer activity. GeneHancer: gradient of red and grey represent promoters and enhancers, respectively, grading from low to high activity.*

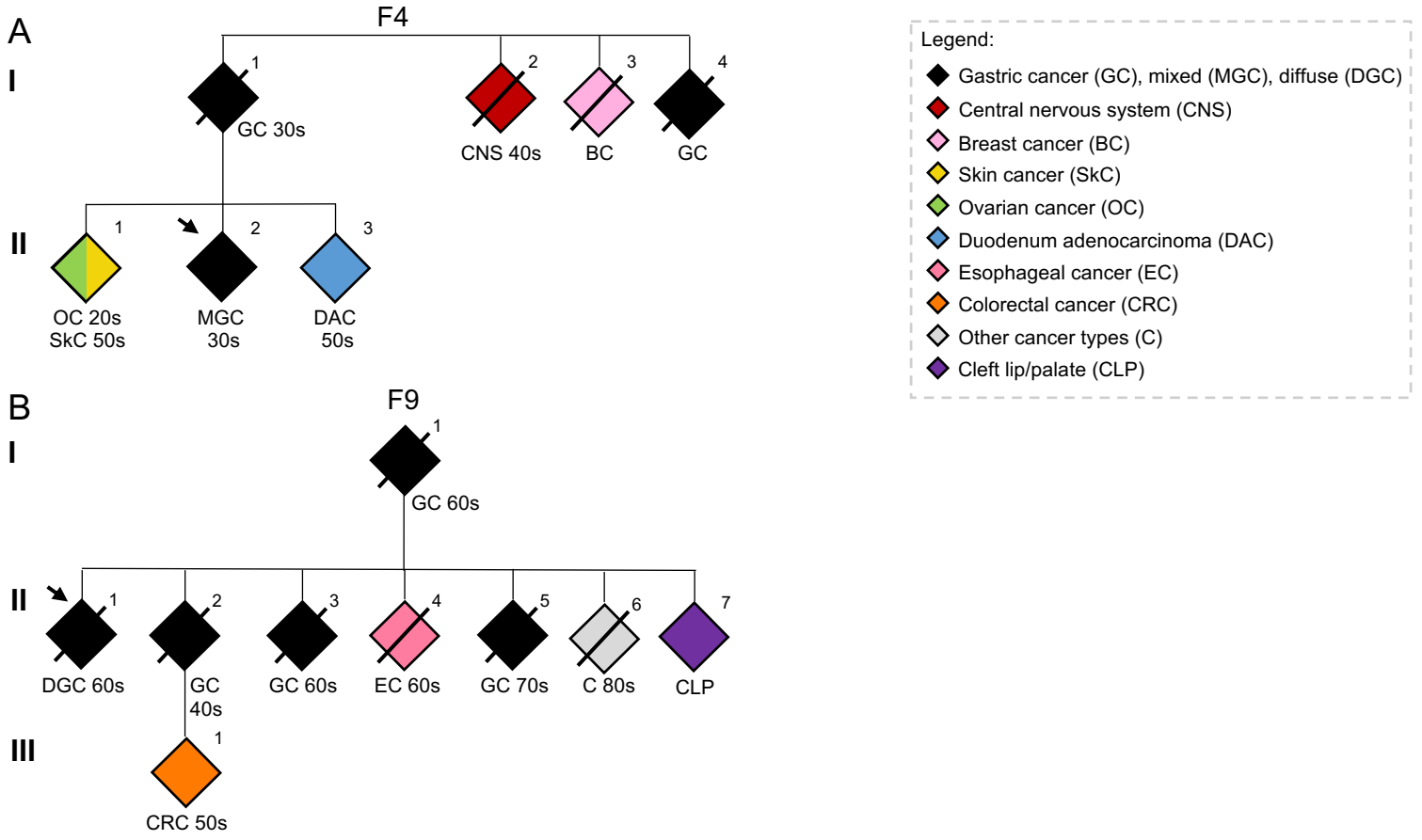


***Figure 2. Family pedigrees.*** *A) Representative family pedigree of F4 carrying the CDH3 CNV, B) Representative family pedigree of F9 carrying the CDH1-TANGO6 intergenic CNV. Black fill represents gastric cancer, red represent central nervous system cancer, light blue represents breast cancer, yellow represent skin cancer, green represent ovarian cancer, grey represent endometrial cancer and blue represent colorectal cancer. Arrow indicates the proband. DGC: diffuse gastric cancer, MGC: mixed gastric cancer, GC: gastric cancer, DAC: adenocarcinoma of the duodenum, CNS: central nervous system cancer, BC: breast cancer, SC: skin cancer, OC: ovarian cancer, EC: Esophageal cancer, CRC: colorectal cancer, CLP: cleft lip/palate.*

A

| Family | Gene | Syndrome | Location hg38 | SV size (bp) | SV type | Perturbed region | AF |
|---|---|---|---|---|---|---|---|
| F15 | *MLH1* | Lynch syndrome | chr3:37039111-37041898 | 2787 | DEL | Intron 13-14, exon 14 | novel |

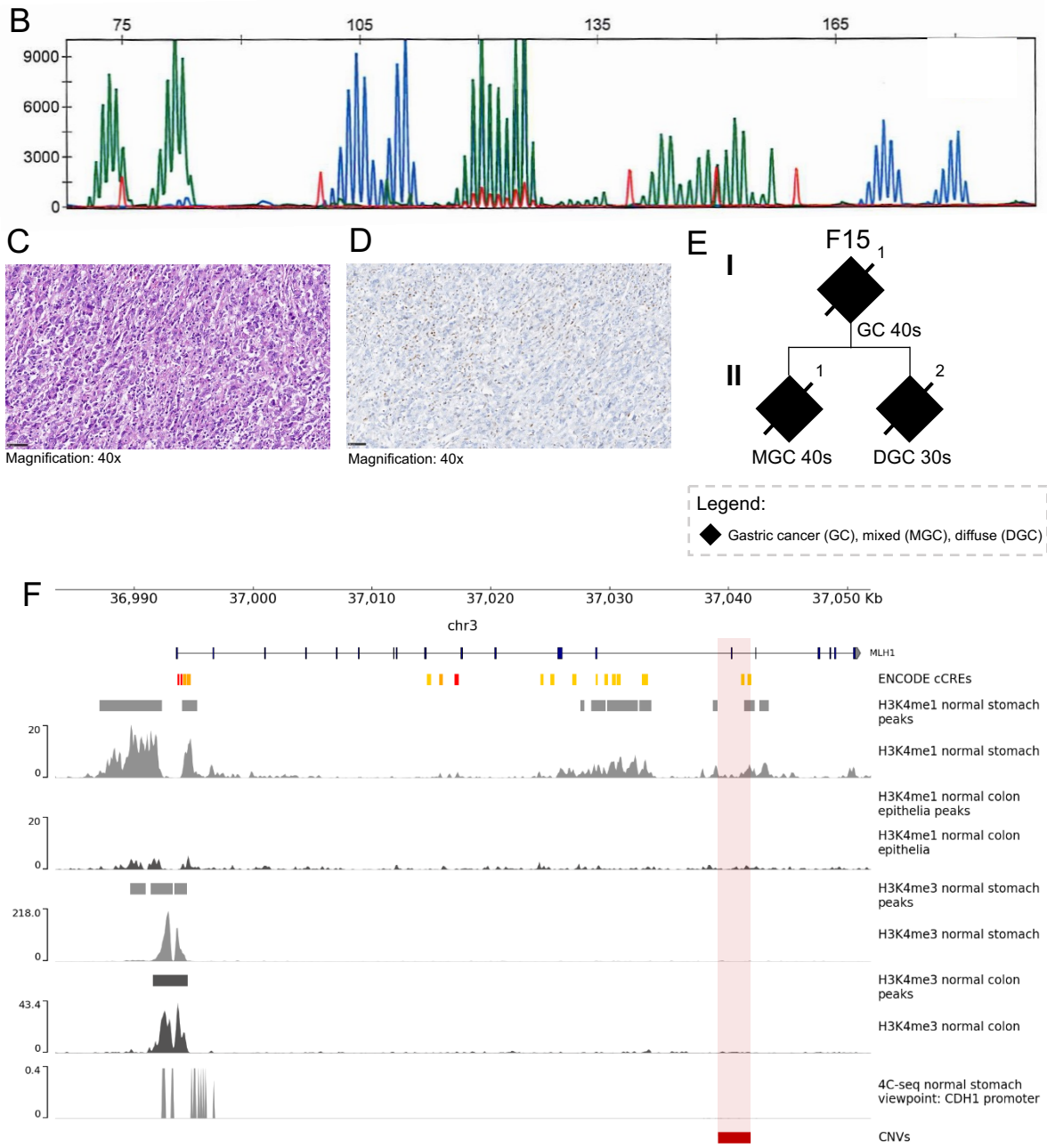


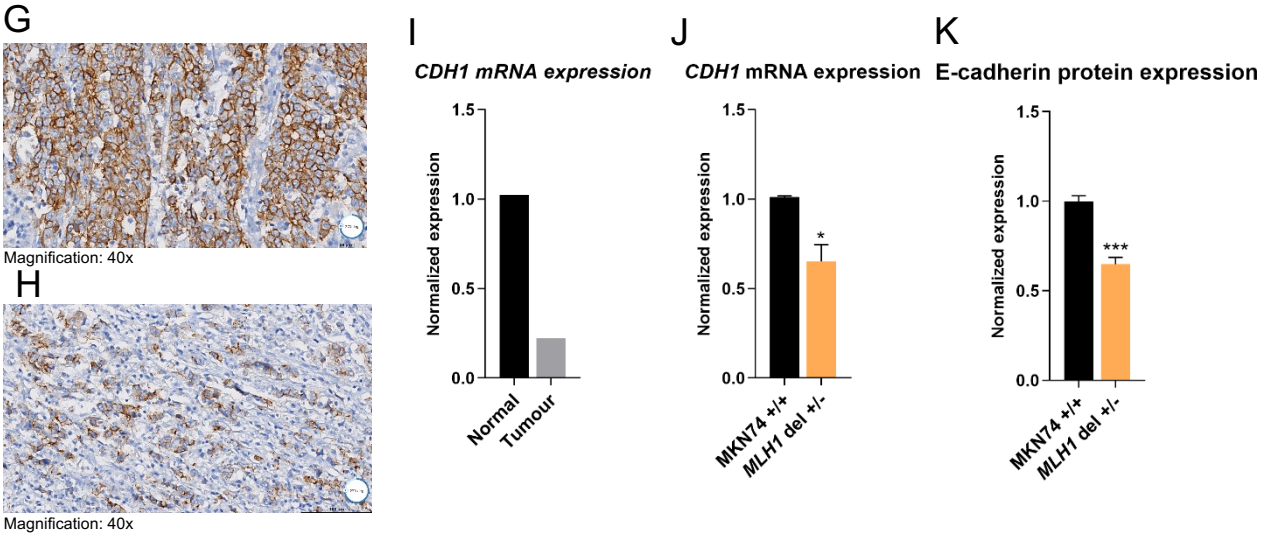


***Figure 3. Genomic CNVs in cancer associated syndromes.*** *A) Description of CNV identified, B) Microsatellite instability (MSI) analysis, C) Hematoxylin and eosin of tumour tissue from proband with MLH1 CNV, D) MLH1 expression of tumour tissue from proband with MLH1CNV (immunohistochemistry), E) Representative family pedigree of F15. Black fill represents gastric cancer development. DGC: diffuse gastric cancer, GC: gastric cancer. F) Chromatin marks and accessibility in normal stomach and colon tissue from ENCODE, G) E-cadherin expression of tumour tissue (intestinal component) from proband with MLH1 CNV (immunohistochemistry), H) E-cadherin expression of tumour tissue (diffuse component) from proband with MLH1 CNV (immunohistochemistry), I) CDH1 mRNA expression in the tumour, J-K) CDH1 mRNA and protein expression of edited MKN74 clones.*

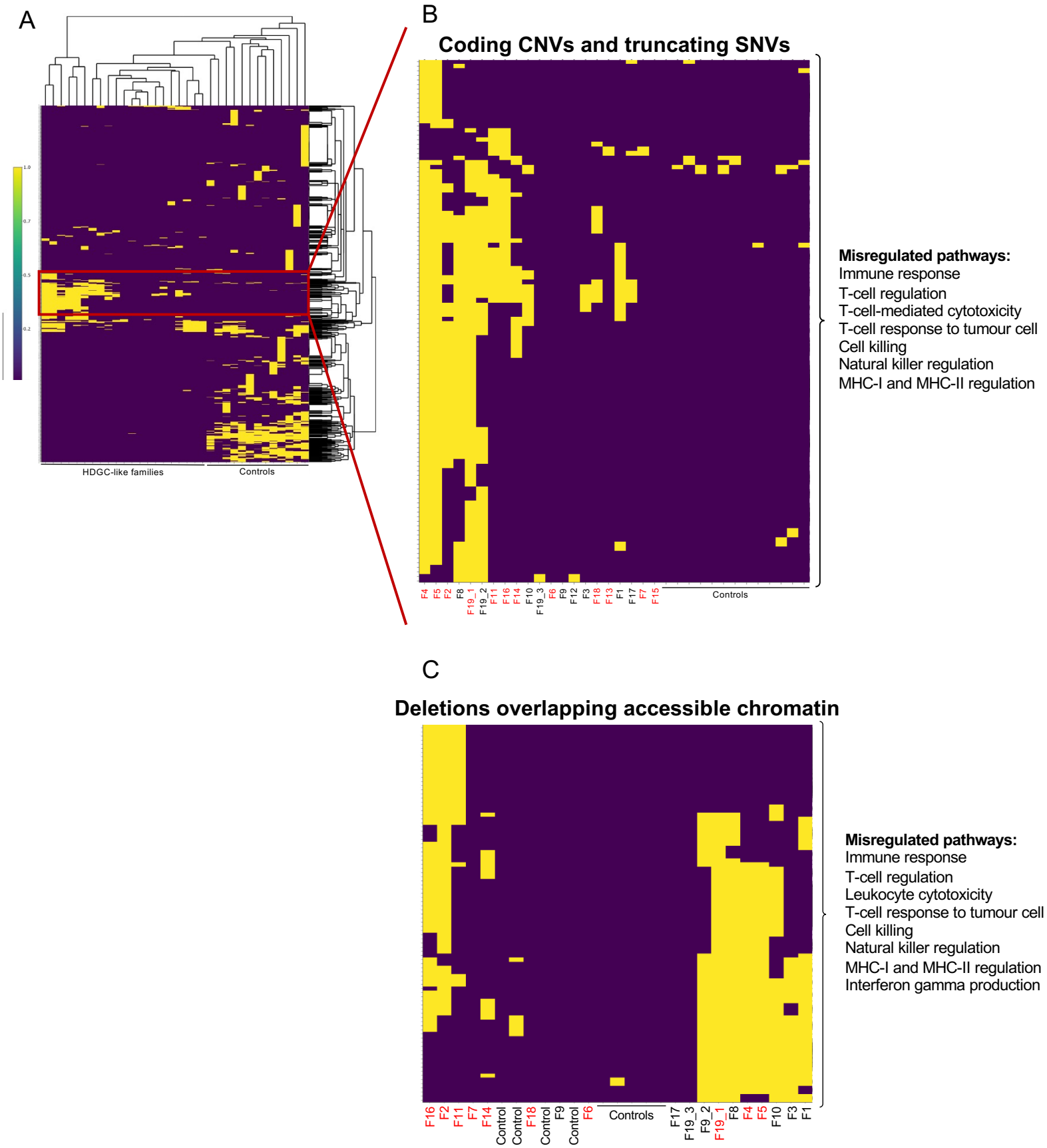


***Figure 4. CNVs and SNVs misregulated pathways in HDGC undiagnosed patients.*** *A) Heatmap representing all impaired pathways in HDGC undiagnosed patients, B) Cluster of immune-associated impaired pathways in HDGC undiagnosed patients and absent in control individuals, C) Cluster of CNVs overlapping accessible chromatin regions in immune-associated pathways. Red represents probands with cancer age of onset ≤50 years of age.*

A

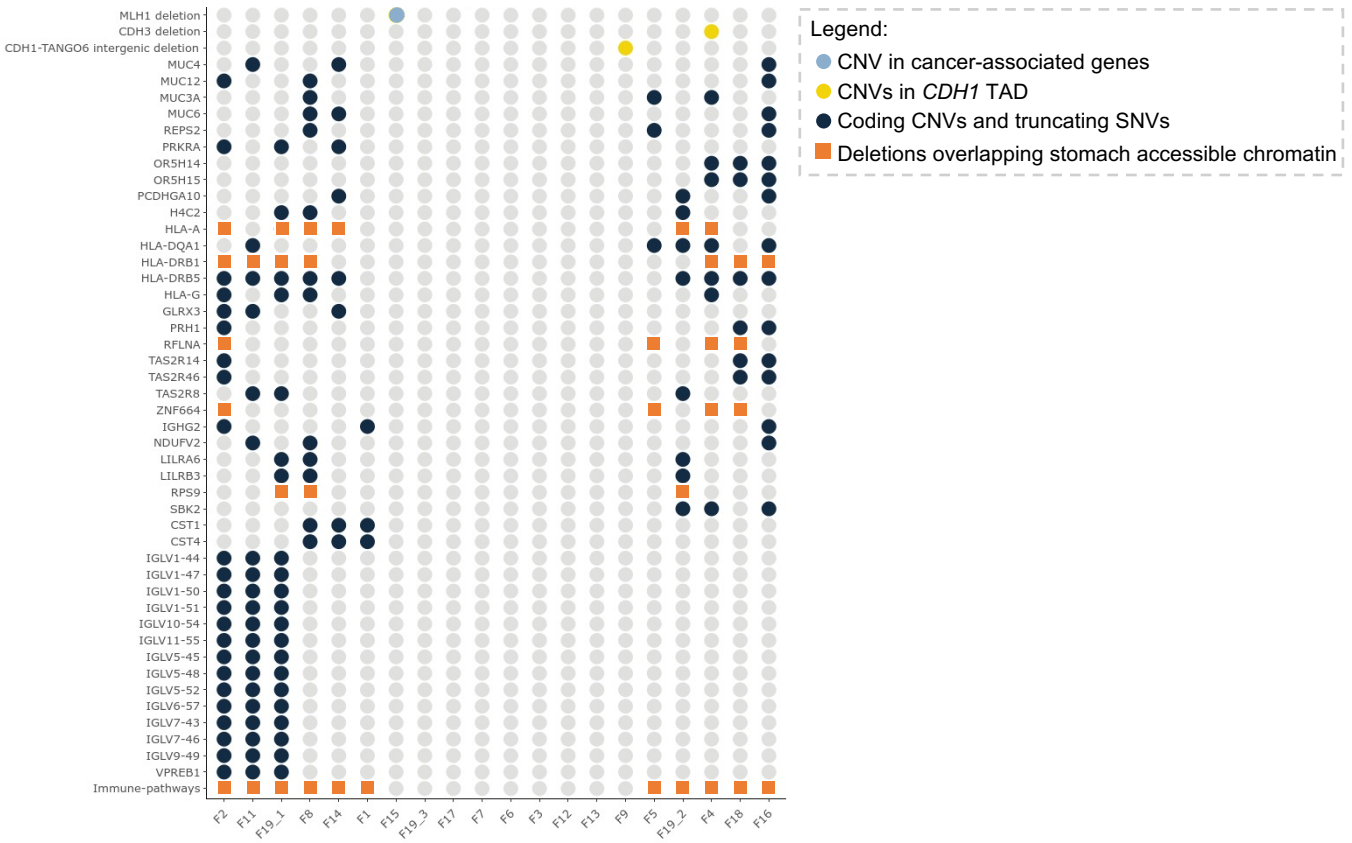


B

| Family | Germline defects | Family history | HDGC 2020 criteria | Meet criteria for other syndromes |
|---|---|---|---|---|
| F15 | MLH1$^{+/-}$ | **MGC 40s**,<br>DGC 30s, GC 40s | 1 | |
| F9 | CDH1-TANGO6 intergenic$^{+/-}$ | **DGC 60s**,<br>GC 60s, GC 40s, GC 60s, ESC 60s, CRC 50s | 1 | |
| F4 | CDH3$^{+/-}$,<br>Immune-related genes | **MGC 30s**,<br>GC 30s, GC 30s, BC, CNS 40s, CRC 30s, Sk 50s, OC 20s | 1 | LS (CRC < 50),<br>HBOC (BC + OC) |
| F5 | Immune-related genes | **DGC 20s,**<br>unknown 50s, unknown 50s | 4 | |
| F16 | Immune-related genes | **DGC 20s**,<br>GC 60s, SARC 70s, Leuk 10s, Sk 40s, 50s | 1 | |
| F19 | Immune-related genes | **IGC 30s, UtC 20s**,<br>*DGC 60s, GC 60s, 60s, **IDC 50s, UtC 50s, BrC , PancC 80s, LC 80s, LC, BIC 60s, 80s, 80s, PC 80s, 80s, BSO, CRC 60s, CRC, CC 20s | 1 | HBOC (BC + PancC) |
| F18 | Immune-related genes | **DGC 30s**,<br>GC 40s, BC 70s, LBC 60s, Lymph 60s | 1 | |
| F2 | Immune-related genes | **DGC 40s**,<br>GC 40s, BC 20s, Sk , HNC, unknown 80s, -, BrC, LC, CRC 40s | 1 | LS (CRC < 50),<br>HBOC (BC < 45) |
| F14 | Immune-related genes | **DGC 40s, BC 40s**,<br>DGC 30s, gastric LMS 30s, IDC 50s, OC or DGC 30s, CRC 30s | 1 | |
| F11 | Immune-related genes | **DGC 40s**,<br>GC 40s, GC 60s, GC, LBC 40s, LBC 50s, IDC 50s, BC 50s, BC | 1, 2, 7 | HBOC (BC < 45) |
| F1 | Immune-related genes | **DGC 60s, PRSC 50s**,<br>GC, GC, GC, 60s, DGC 60s, BC 70s, MM 70s, OC 30s, CRC 40s, NHL 20s | 1 | |
| F8 | Immune-related genes | **MGC 70s**,<br>GC 30s, GC 70s, PC 60s, CRC 70s | No | |
| F6 | | **DGC 30s**,<br>DGC 30s, Leuk 60s, BIC 60s, PancC 70s, OC 40s | 1 | |
| F13 | | **DGC 40s**,<br>DGC 40s, GC 70s, BC, BIC, LC 60s, 60s, 50s, PC 70s, 70s, Sk 50s, CC | 1 | |
| F17 | | **DGC 50s**,<br>GC 40s, BC 70s, CRC 80s, RC, BoC | 1 | |
| F7 | | **DGC 50s**,<br>GC 80s, IDC 50s, CRC, CRC, CRC, CRC | 4 | LS (>3 CRCs) |
| F12 | | **DGC 50s**,<br>GC 40s, CRC 80s, 50s, ESC 70s | 1 | |
| F10 | | **LBC 60s**,<br>GC 50s, GC 80s, GC, BC 50s, PancC, HNC , MM 40s, TC 40s | No | HBOC (BC + PancC) |
| F3 | | **DGC 60s**,<br>GC 30s, GC 70s, MGC 70s, PRSC 60s, LC smoker 50s, CRC 70s | 1 | |

***Figure 5. Main findings solving the missing heritability in HDGC patients.*** *A) Heatmap representing misregulated genes in HDGC undiagnosed families, Blue represents ultra-rare (AF<0.00001) coding CNVs and truncating SNVs found from WGS sequencing of HDGC patients. Yellow represent CNVs found overlapping CDH1 TAD. Orange square represents pathways overlapping accessible chromatin in normal stomach, B) Description of the genetic defects, family history, clinical criteria and ancestry of HDGC undiagnosed families. GC: gastric cancer, DGC: diffuse gastric cancer, BC: breast cancer, LBC: lobular breast cancer, PRSS: prostate cancer, MGC: mixed-type gastric cancer, IGC: intestinal gastric cancer, IDC: invasive ductal breast cancer, CRC: colorectal cancer, EsoC: esophageal cancer, RC: renal cancer, Panc: pancreatic cancer, BldC: blader cancer, Sarc: sarcoma, OvC: ovarian cancer, Cerv: cervical cancer, UtC: uterine cancer, SkC: skin cancer, MM: melanoma, BrC: CNS: central nervous system cancer, HN: head and neck, Leuk: leukemia, NHL: non-hodkins lymphoma, Lymp: lymphoma, LC: lung cancer. In F19, * represent phenotype in individual F19_2 and ** represent phenotype in individual F19_3.*